Drug Design, Development and Therapy

Dovepress

open access to scientific and medical research

Open Access Full Text Article

ORIGINAL RESEARCH

Synergistic Effect of Tangeretin and Atorvastatin for Colon Cancer Combination Therapy: Targeted Delivery of These Dual Drugs Using RGD Peptide Decorated Nanocarriers

This article was published in the following Dove Press journal:
Drug Design, Development and Therapy

He Bao[1,*]
Nanbo Zheng[2,*]
Zhuanting Li[1]
Yuan Zhi[3]

[1]Department of Pharmacy, The Second Affiliated Hospital of Xi'an Jiaotong University, Xi'an 710004, People's Republic of China; [2]Department of Pharmacy, Xi'an Central Hospital, Xi'an 710003, People's Republic of China; [3]Department of Pharmacy, Xi'an Hospital of Traditional Chinese Medicine, Xi'an 710021, Shaanxi, People's Republic of China

*These authors contributed equally to this work

Purpose: Colorectal cancer (CRC) is the third most frequently diagnosed cancer and the fourth leading cause of cancer death over the world. Nano-sized drug delivery systems are used for the treatment of cancers. The aim of this study was to develop a tangeretin (TAGE) and atorvastatin (ATST) combined nano-system decorated with RGD (RGD-ATST/TAGE CNPs) for colon cancer combination therapy.

Materials and Methods: In this study, cyclized arginine-glycine-aspartic acid sequences (RGD) contained ligand was synthesized by conjugating cyclo (Arg-Gly-Asp-d-Phe-Lys) (cRGDfK) with D-α-tocopheryl succinate dichloromethane (TOSD) using polyethylene glycol (PEG) as a linker to obtain cRGDfK-PEG-TOSD. ATST and TAGE combined nano-systems: RGD-ATST/TAGE CNPs were prepared. The combination effects as well as antitumor effects of these two agents were evaluated on colon cancer cells and mice bearing cancer models.

Results: Drug entrapment efficiencies of nano-systems were high (around 90%), suggesting the good loading capacity. The release profiles of ATST or TAGE from RGD-ATST/TAGE CNPs followed Higuchi model. The RGD-decorated nano-system showed more obvious cytotoxicity on HT-29 cells than the undecorated nano-system, but no obvious difference was found on normal CCD-18 cells. The strongest synergism was observed when the weight ratio of ATST to TAGE was 1:1. In vivo biodistribution of RGD-ATST/TAGE CNPs in the tumor site is high and prominently inhibited the in vivo tumor growth.

Conclusion: The results demonstrated that RGD-ATST/TAGE CNPs showed the most significant synergistic therapeutic efficacy, exhibited no significant toxicity to major organs and tissues, and body weight of the treated mice was stable. Therefore, the combination nano-system is a promising platform for colon cancer therapy.

Keywords: colorectal cancer, tangeretin, atorvastatin, nanoparticles, cytostatic anticancer agents

Introduction

Colorectal cancer (CRC) is the third most frequently diagnosed cancer and the fourth leading cause of cancer death over the world.[1] In 2030, with an expected 60% increases of CRC, an estimated more than 2.2 million new cases and 1.1 million cancer deaths will occur.[1] Approximately 50–60% of patients diagnosed with CRC develop colorectal metastases, and 80–90% of these patients have unresectable liver metastases, therefore, systemic or chemo-therapy for advanced,

Correspondence: Nanbo Zheng
Department of Pharmacy, Xi'an Central Hospital, 185 Houzai Men, Xi'an 710003, People's Republic of China
Email zhengnbxju@163.com

submit your manuscript | www.dovepress.com
DovePress
http://doi.org/10.2147/DDDT.S256636

recurrent, or metastatic colon cancer remains an important approach and the focus of clinical treatment.[2,5] Based on National Comprehensive Cancer Network (NCCN) guidelines of colon cancer (version 1.2020), cytotoxic anticancer drugs including fluoropyrimidine, irinotecan, oxaliplatin, leucovorin, and so on have still been recommended because of their cell-death mechanism to colon cancer cells. However, this cell-death not only acts on the tumor but also normal, non-tumor tissues, which results in severe toxicity, and this cell-death without targeting is faced with multidrug resistance (MDR) that seriously hinders therapeutic efficacy.[6,8]

The role of polymethoxylated flavones (natural substances) has come into the spotlight recently because of their cytostatic anticancer mechanism bringing in lower cytotoxicity and anti-MDR ability.[9,11] Tangeretin (TAGE), belonging to polymethoxylated flavones from citrus fruits, has been proven to inhibit colon cancer cell proliferation and hepatocellular carcinoma proliferation in vitro and in vivo that brings a benefit for colorectal metastases and unresectable metastatic liver metastases.[12,14] TAGE exhibits its anticancer activity through inducing G_1 cell-cycle arrest, regulating gene transcription, and inhibiting P-glycoprotein.[15,16] Despite its excellent anticancer efficacy, its clinical application is hurdled by low aqueous solubility and poor oral absolute bioavailability (mean value <3.05%).[17]

Atorvastatin (ATST) is a synthetic statin commonly used in the treatment of hypercholesterolemia.[18] ATST was also reported as having the ability to modulate cell apoptosis, thus influencing a wide range of diseases including cancer.[19] Accumulating studies have shown that a combination of ATST with different agents produced enhanced anti-cancer effects against various cancers, including colon, lung, and prostate cancer.[20] Examples included a combination of ATST and celecoxib synergistically induces cell cycle arrest and apoptosis in colon cancer cells;[21] ATST potentiates the anti-angiogenic effects of bevacizumab in human colorectal cancer.[22] In this study, the combination of ATST with TAGE was applied for the colon cancer therapy.

The αvβ3 integrin receptor is specifically overexpressed in some tumor cells and has been implicated in the promotion of tumor growth, progression, and metastasis of solid tumors.[23] A number of synthetic cyclized arginine-glycine-aspartic acid sequences (RGD) containing peptides have been identified to have high affinity with integrin αvβ3.[24] So conjugates containing RGD motif were in synthesized and utilized for drug delivery to cancers.[25] Nano-sized drug delivery systems are used for the diagnosis and treatment of cancers.[26] RGD modified nano-systems were proved to be efficient for colon carcinoma treatment.[27,28]

In the present research, we constructed RGD modified, ATST and TAGE combined nano-systems. Firstly, a new RGD-containing ligand was synthesized. Then a novel nano-system was designed for the co-loading of two drugs. The combination effects as well as antitumor effects of these two agents were evaluated on colon cancer cells and mice bearing cancer models.

Materials and Methods

Materials

Cyclo (Arg-Gly-Asp-d-Phe-Lys) (cRGDfK) and polyethylene glycol (PEG) were purchased from Xi'an ruixi Biological Technology Co, Ltd (Xi'an, China). D-α-tocopheryl succinate dichloromethane (TOSD) was obtained from Shanghai ZZBIO Co., Ltd (Shanghai, China). Dicyclohexylcarbodiimide (DCC), glyceryl monostearate (GMS), Carbopol 940 (CBP), 3-(4,5-dimethylthiazole-2-yl)−2,5-diphenyltetrazolium bromide (MTT), and Dulbecco's modified Eagle's medium (DMEM) were obtained from Sigma-Aldrich (St. Louis, MO). Fetal bovine serum (FBS) was provided by Lonza Bioscience (Walkersville, MD).

Synthesis of RGD-Containing Ligand

RGD-containing ligand was synthesized by conjugating cRGDfK with TOSD using PEG as a linker to obtain cRGDfK-PEG-TOSD (Figure 1).[29,30] TOSD (1.2 equivalents) and PEG (1 equivalent) were dissolved in dichloromethane, then DCC (1.1 equivalents) was added drop by drop in an ice bath, stirred at 25°C overnight (mixture 1). cRGDfK (1.2 equivalents) was then added along with DCC (1.1 equivalents) to the mixture 1. After reacting at 25°C overnight, the mixture was put into a rotary evaporator to remove the dichloromethane, cRGDfK-PEG-TOSD was separated by filtration, washed three times with ethyl ether, and obtained by vacuum drying overnight with a production rate of 81.2%.[31] The chemical structure of cRGDfK-PEG-TOSD was confirmed ^{1}H NMR.

Construction of Nano-Systems

ATST loaded lipid nanoparticles (ATST LNPs, Figure 2) were prepared by solvent displacement method.[32] ATST (50 mg) and GMS (100 mg) were dissolved in acetone

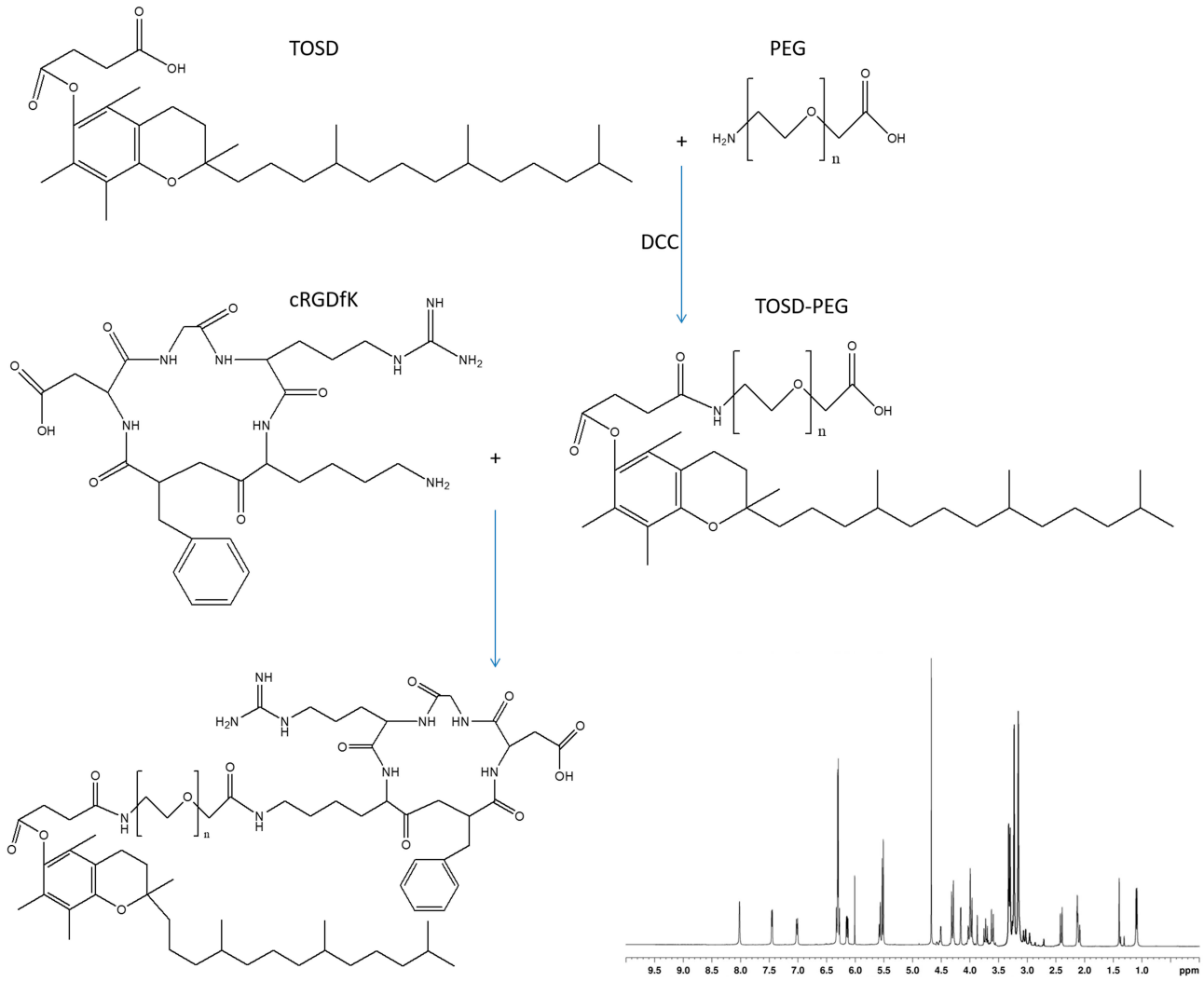

Figure 1 RGD contained ligand was synthesized by conjugating cRGDfK with TOSD using PEG as a linker to obtain cRGDfK-PEG-TOSD. The chemical structures of cRGDfK-PEG-TOSD was confirmed ^{1}H NMR.

(5 mL), and added into distilled water (15 mL, contained 0.5% DDAB) under stirring (400 rpm). ATST LNPs was collected by centrifugation (10,000×g, 30 min) and washed three times with distilled water.

TAGE loaded zein nanoparticles (TAGE ZNPs, Figure 2) were prepared using a liquid–liquid dispersion method.[33] TAGE (50 mg) and zein (100 mg) were dissolved in acetone (5 mL), and added into distilled water (15 mL, contained

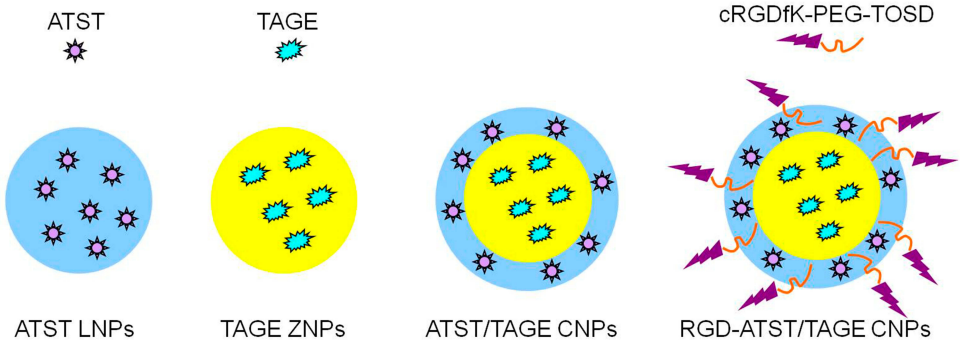

Figure 2 Construction of nano-systems: ATST LNPs, TAGE ZNPs, ATST/TAGE CNPs, and RGD-ATST/TAGE CNPs.

0.05% CBP) under stirring (400 rpm). TAGE ZNPs were collected by centrifugation (10,000×g, 30 minutes) and washed three times with distilled water.

ATST and TAGE combined nano-systems (ATST/TAGE CNPs, Figure 2) were prepared by combining the above two methods. TAGE ZNPs was firstly prepared and then added into distilled water (mixture 2). ATST (50 mg) and GMS (100 mg) were dissolved in acetone (5 mL), and added into mixture 2 under stirring (400 rpm).

RGD modified, ATST and TAGE combined nano-systems (RGD-ATST/TAGE CNPs, Figure 2) were prepared by adding cRGDfK-PEG-TOSD to the ATST/TAGE CNPs under stirring (400 rpm). Blank RGD modified, ATST and TAGE combined nano-systems (RGD CNPs) without drugs were prepared by the similar method without adding ATST and TAGE.

All the above mentioned nano-systems were lyophilized and stored at 4°C until further analysis.

Particle Size and Zeta Potential

Particle size, polydispersity index, and zeta potential of nano-systems were characterized by Dynamic Light Scattering (DLS, Beckman Coulter Delsa Nano C, Fullerton, CA) at 25°C.[34]

Drug Entrapment Efficiency and Release Kinetics

Drug entrapment efficiency was determined by the separation of the drugs from the nano-systems by ultracentrifugation (15,000×g, 30 minutes, 4°C).[35] The concentration of ATST was determined by measuring the absorbance at 246 nm using a UV-VIS spectrophotometer. The dosage of TAGE was evacuated by HPLC method.[36] Diamonsil C18 column (250 mm×4.6 mm, 5 μm) was used along with water-methanol (4:6, v/v) mobile phase. The flow rate was 1.0 mL/min and the detection wavelength was 326 nm.

Release studies were operated by dialysis method using dialysis bags (molecular weight cut off 10,000). Nano-systems were sealed in the bags separately and suspended in a beaker containing phosphate buffer saline (PBS, 0.1 M, pH 7.4, 100 mL) under stirring (100 rpm). At preset time intervals, the release medium (2 mL) was taken out and analyzed for drug release by the same method as "drug entrapment efficiency". The same amount of fresh PBS (2 mL) was replenished into the release medium. The drug release behaviors were fitted into zero-order, first order, matrix, Hixon-Crowell cube root law and Korsmeyer-Peppas models to select the most appropriate model.

Cells

Human colon cancer cell lines HT-29 (HT-29 cells), SW480 (SW480 cells); and the normal human colon CCD-18 cell line (CCD-18 cells) were obtained from the American Type Culture Collection (ATCC, Manassas, VA). The cell lines were maintained in a humidified 5% CO_2 incubator using DMEM supplemented with 10% FBS, 1% of antibiotics mixture of penicillin (10,000 U/mL), and streptomycin (10 mg/mL).[37]

MTT Assay and Combination Index Calculation

HT-29 cells, SW480 cells, and CCD-18 cells were seeded in 24-well plates (1×10^4 cells/well) in 300 μL of supplemented DMEM. MTT assay was used to determine the cytotoxic effects of nano-systems against cancer or normal cells.[38] Briefly, after 24 hours of culture, the cells were treated with drug-loaded nano-systems and free drugs at certain concentrations for 24 hours. Subsequently, MTT was added to the treated cells for 3 hours, with added DMSO, and then placed in the cells for 15 minutes. Finally, the absorbance at 570 nm was measured. The half maximal inhibitory concentration (IC_{50}) values of all the formulations were calculated.

The combination index (CI) values were determined by IC_{50} and calculated by the median-effect equation as described by Chou and Talaly[39,40] and Palko-Łabuz et al. The value of CI<1 represents drug synergy, CI>1 indicates drug antagonism, while an additive effect is observed when CI=1.

Animals

Female BALB/c mice (6-weeks-old) were purchased from the Laboratory Animal Center of Xi'an Jiaotong University. HT-29 cells (4×10^5 cells in 0.2 mL of cell suspension) were injected subcutaneously into the right fossa axillaris of nude mice to produce a colon cancer xenograft. All the experiments followed the National Institutes of Health guidelines for the care and use of laboratory animals and approved by the Medical Ethics Committee of Xi'an Central Hospital (No. 20200323(1)).

In vivo Biodistribution

Colon cancer xenografts were randomly divided into seven groups and received injections of RGD-ATST/TAGE CNPs,

ATST/TAGE CNPs, ATST LNPs, TAGE ZNPs, RGD CNPs, free ATST/TAGE (each contained 5 mg/kg of ATST and/or TAGE), and 0.9% saline as control.[41] Mice were sacrificed after 1 hour of administration, and tumor, heart, kidney, liver, lung, and spleen were harvested. Tissues were homogenized with saline (containing 1 mM EDTA) to prepare 20% (w/v) homogenate solution. Ethanol was firstly added followed by adding hexane/diethyl ether (3:1, v/v) to extract the drugs from the tissues. The extract was centrifugated (1000×g, 10 minutes, 4°C), the upper layer was collected, and it was analyzed by the methods described in the "Drug Entrapment Efficiency" section.

In vivo Pharmacokinetics

The same procedure was carried out as in the above "In vivo Biodistribution" section. Blood samples of mice were collected in heparinized tubes at 0.25, 0.5, 0.75, 1, 2, 3, 4, 5, and 6 hours. Plasma was isolated from whole blood by centrifugation (1000×g, 10 minutes), then the separated plasma was spun with triple methanol in a centrifuge tube for 30 seconds and centrifuged (1000×g, 5 minutes). The drugs existing in samples of plasma were analyzed by the methods in the "Drug Entrapment Efficiency" section.

In vivo Anti-Tumor Efficacy

Seven groups of colon cancer xenografts received the injections of RGD-ATST/TAGE CNPs, ATST/TAGE CNPs, ATST LNPs, TAGE ZNPs, RGD CNPs, free ATST/TAGE (each containing 5 mg/kg of ATST and/or TAGE), and 0.9% saline as control every other day for 14 consecutive days. During the treatment, tumor size was measured every 4 days. Tumor volumes were calculated and a tumor growth curve was plotted. Mice were sacrificed by cervical dislocation on day 20 and the tumor tissues were collected, captured, and weighted. The tumor inhibition rate on day 20 was calculated.

Statistical Analysis

The non-parametric data was analyzed using Friedman test. $P<0.05$ was considered statistically significant.

Results

Characterization of cRGDfK-PEG-TOSD

The chemical structure of cRGDfK-PEG-TOSD was confirmed by ^{1}H NMR (Figure 1). ^{1}H NMR ($CDCl_3$, 500 MHz) δ: 1.01 (CH_3 of TOSD), 1.43 (CH_2 of TOSD), 2.12 (NH_2 of cRGDfK), 2.41 (CH_3 in the benzene ring of TOSD), 3.36 (CH_2 of PEG), 3.69 (CH_2 of cRGDfK), 4.26 (CH_2 next to the amide linkage), 4.61 (CH_2 of cRGDfK), 6.33 (NH of cRGDfK), 7.02 (H in the benzene ring of cRGDfK), 7.46 (NH of cRGDfK), and 8.02 (NH of the amide linkage).

Particle Size and Zeta Potential of Nano-Systems

Particle sizes of ATST LNPs and TAGE ZNPs were 102.4 and 113.6 nm, which were a little bit higher than 100 nm (Figure 3). For the double layered ATST/TAGE CNPs, size increased to 132.6 nm. RGD decorated CNPs showed the largest diameter of 156.9 nm (RGD-ATST/TAGE CNPs) and 153.8 nm (RGD CNPs). ATST LNPs (19.3 mV) and TAGE ZNPs (−33.5 mV) exhibited opposite zeta potential. When ATST/TAGE CNPs were constructed using zein as the surface layer, zeta potential was negative (−23.2 mV), however, with the presence of RGD, the surface charge increased to −17.1 mV (RGD-ATST/TAGE CNPs).

Drug Entrapment Efficiency and Release Kinetics

Table 1 summarized the drug entrapment efficiencies of nano-systems, which were all around 90%. The release profiles of ATST or TAGE from the nano-systems are presented in Figure 4. Faster release of ATST was found than that of

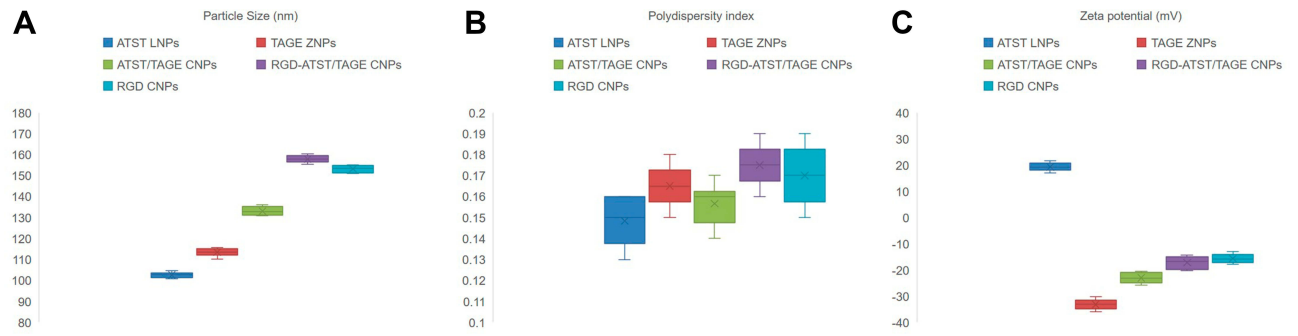

Figure 3 Particle size (**A**), polydispersity index (**B**), and zeta potential (**C**) of nano-systems.

Table 1 Drug Entrapment Efficiency of Nano-Systems

Formulation	ATST LNPs	TAGE ZNPs	ATST/ TAGE CNPs	RGD-ATST /TAGE CNPs
ATST entrapment efficiency (%)	92.1 ±2.2	/	90.3±3.1	91.3±3.7
TAGE entrapment efficiency (%)	/	92.2 ±2.9	88.9±4.1	89.3±3.6

Abbreviations: ATST, atorvastatin; LNPs, lipid nanoparticles; TAGE, tangeretin; ZNPs, zein nanoparticles; RGD, arginine-glycine-aspartic; CNPs, combined nano-systems.

TAGE from ATST/TAGE CNPs, which could be attributed to the different location of the two drugs. ATST was in the outer layer of the nano-system and will be released easier.

Cytotoxicities and Combination Index Calculation

Cytotoxicities of both nano-systems and free drugs exhibited a dose dependent manner on HT-29 cells, SW480 cells, and CCD-18 cells (Figure 5). However, similar cell viability of nano-systems and free drugs was found on CCD-18 cells. On the opposite, formulations showed different effects on HT-29 cells. For example, ATST/TAGE CNPs significantly inhibited the HT-29 cells viability than that of free ATST/TAGE (P<0.05). RGD decorated nano-system showed an obvious cytotoxicity on HT-29 cells compared to an undecorated nano-system, but no obvious difference was found on normal CCD-18 cells. This could be the evidence that RGD may enhance the target ability of the nano-system thus gain better tumor cell inhibition effects. The CI values obtained for HT-29 cells indicated a synergistic effect in case of the drugs combination in the nano-systems (Table 2). In Table 2, CI values of ATST LNPs and TAGE ZNPs were presented and ATST/TAGE CNPs with different ATST to TAGE rations all illustrated synergy effects. The strongest synergism (CI=0.3465) was observed when the ratio was 1:1 (ATST to TAGE, w/w). So the same amount of drugs was used during the preparation of the nano-systems.

In vivo Biodistribution and Pharmacokinetics

The concentrations of drugs in the tumor site showed significant differences (Figure 6). RGD-ATST/TAGE CNPs exhibited the highest tumor distribution, which is higher than ATST/TAGE CNPs (P<0.05). ATST/TAGE CNPs also accumulated more in the tumor than free

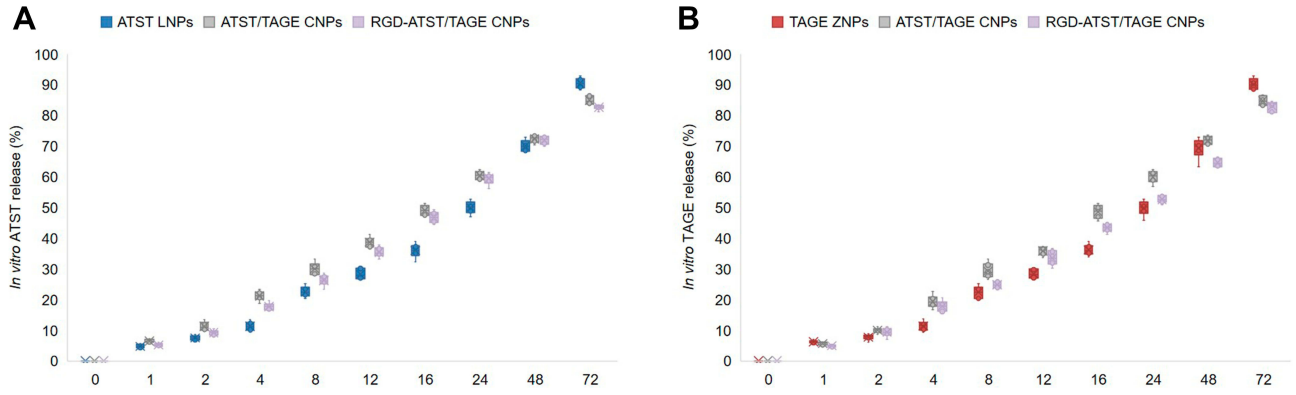

Figure 4 The release profiles of ATST (**A**) or TAGE (**B**) from ATST LNPs and TAGE ZNPs.

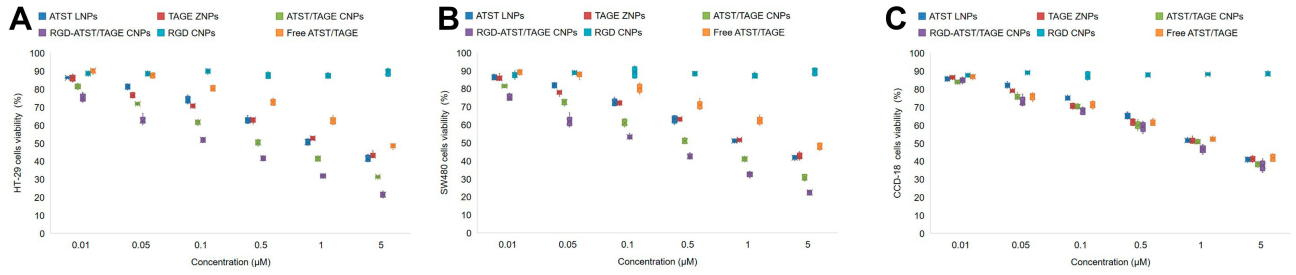

Figure 5 Cytotoxicities of both nano-systems and free drugs exhibited a dose dependent manner on HT-29 cells (**A**), SW480 cells (**B**), and CCD-18 cells (**C**).

Table 2 CI Values Obtained for HT-29 Cells

ATST:TAGE Ratios	10:1	5:1	2:1	1:1	1:2	1:5	1:10
CI values	0.7385	0.5644	0.5232	0.3465	0.4986	0.6153	0.8418

Abbreviations: CI, combination index; ATST, atorvastatin; TAGE, tangeretin.

ATST/TAGE (P<0.05). Increased levels of drugs were found in heart and kidney by free ATST/TAGE; in contrast, drugs loaded in nano-systems showed lower distribution in these organs (P<0.05). Taken together, these results suggest that RGD decorated nano-systems could quickly transfer the drugs to the tumor tissue and avoid high accumulation in the heart and kidney. The blood concentration-time profiles showed that free drugs were rapidly removed from the circulation in comparison with the nano-systems. The drugs concentration remained high in the blood for a longer period of time when they were carried by nanoparticles. RGD-ATST/TAGE CNPs and ATST/TAGE CNPs showed the most remarkable ability to remain the drugs concentrations. The pharmacokinetic parameters are summarized in Table 3. The area under the concentration-time curve (AUC) for RGD-ATST /TAGE CNPs was greater than that for ATST/TAGE CNPs (1.96 times for ATST and 2.26 times for TAGE). The significant increase in half-life indicates that the elimination of nano-systems was slower and that the circulation time was longer than free drugs.

In vivo Anti-Tumor Efficacy

In vivo anti-tumor efficacy of the nano-systems was evaluated by measuring and plotting the curve of the tumor volume after treatment (Figure 7). The tumor volume growth of the drugs treated groups was more modest compared to the control group. At day 20, the tumor volume of the RGD-ATST/TAGE CNPs group (212.4 ±26.7 mm^3) was significantly smaller than the ATST/TAGE CNPs group (302.3±34.9 mm^3) (P<0.05). The ATST/TAGE CNPs group showed smaller tumor volume than the ATST LNPs group (383.1±39.5 mm^3, P<0.05), the TAGE ZNPs group (390.8±35.7 mm^3, P<0.05), and free ATST/TAGE (712.3±46.7 mm^3, P<0.05). The Free ATST/TAGE group exhibited better tumor inhibition efficiency than the control group (915.2±59.6 mm^3, P<0.05). The tumor inhibition rates for RGD-ATST/TAGE CNPs, ATST/TAGE CNPs, ATST LNPs, TAGE ZNPs, and free ATST/TAGE were 76.8%, 66.9%, 58.1%, 57.3%, and 22.2%, respectively (Table 4). There were no significant differences in the body weight of mice before and after treatment (data not shown).

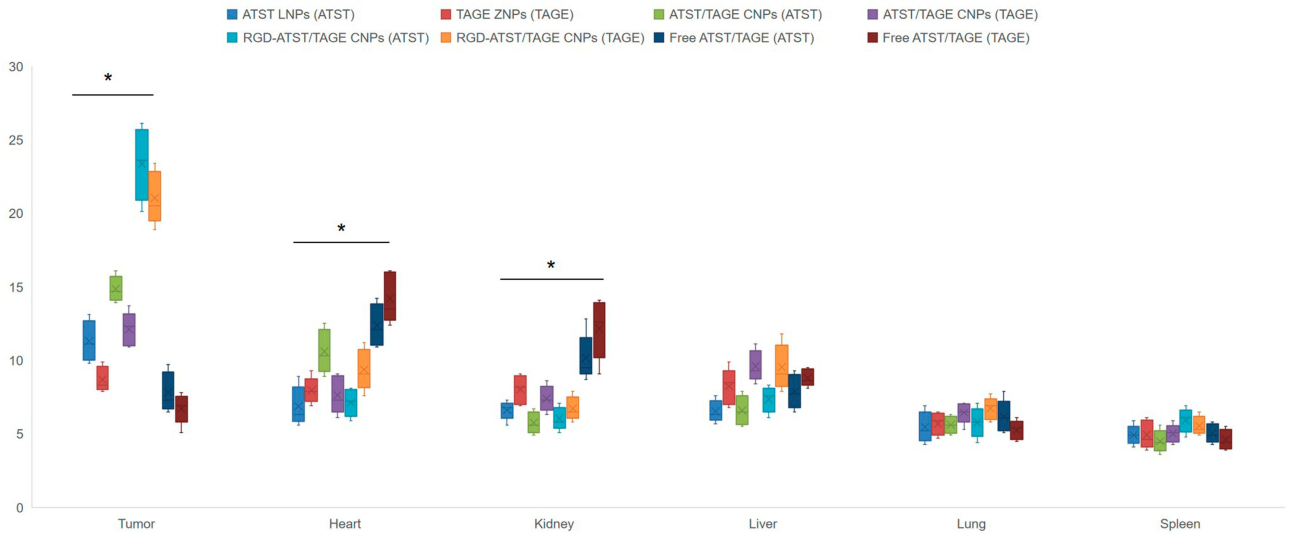

Figure 6 In vivo biodistribution of ATST (presented as (ATST) behind the nano-systems) or TAGE (presented as (TAGE) behind the nano-systems) in the tumor site and other organs. * P<0.05.

Table 3 The Pharmacokinetic Parameters

Parameters	Drugs	Free ATST/ TAGE	ATST/ TAGE CNPs	RGD-ATST /TAGE CNPs
C_{max} (L/kg/h)	ATST TAGE	19.5±1.5 17.6±1.7	20.1±1.9 18.7±1.8	21.3±2.6 18.3±1.5
$T_{1/2}$ (h)	ATST TAGE	1.5±0.3 1.3±0.2	5.8±0.9* 7.9±0.7*	9.3±1.1* 11.3±0.9*
AUC (mg/L. h)	ATST TAGE	35.9±2.8* 30.3±3.1*	156.8±8.9* 128.3±6.7*	307.6±19.8* 289.5±13.7*

Note: *P<0.05 compared with Free ATST/TAGE.
Abbreviations: C_{max}, plasma drug peak concentration; $T_{1/2}$, half-life of drugs; AUC, area under the curve.

Discussion

The aim of this study was to develop a tangeretin and atorvastatin combined nano-system decorated with RGD for colon cancer combination therapy. Studies have been carried out by researchers including the evaluation of the combined effects of berberine and evodiamine on colorectal cancer cells in vitro,[42] and curcumin synergized the action of 5-fluorouracil and oxaliplatin against chemoresistant human cancer colon cells.[43] RGD peptide decorated nanocarriers have been widely used as delivery systems for targeted anti-cancer chemotherapy,[44] and also applied for combinatorial topotecan and quercetin delivery

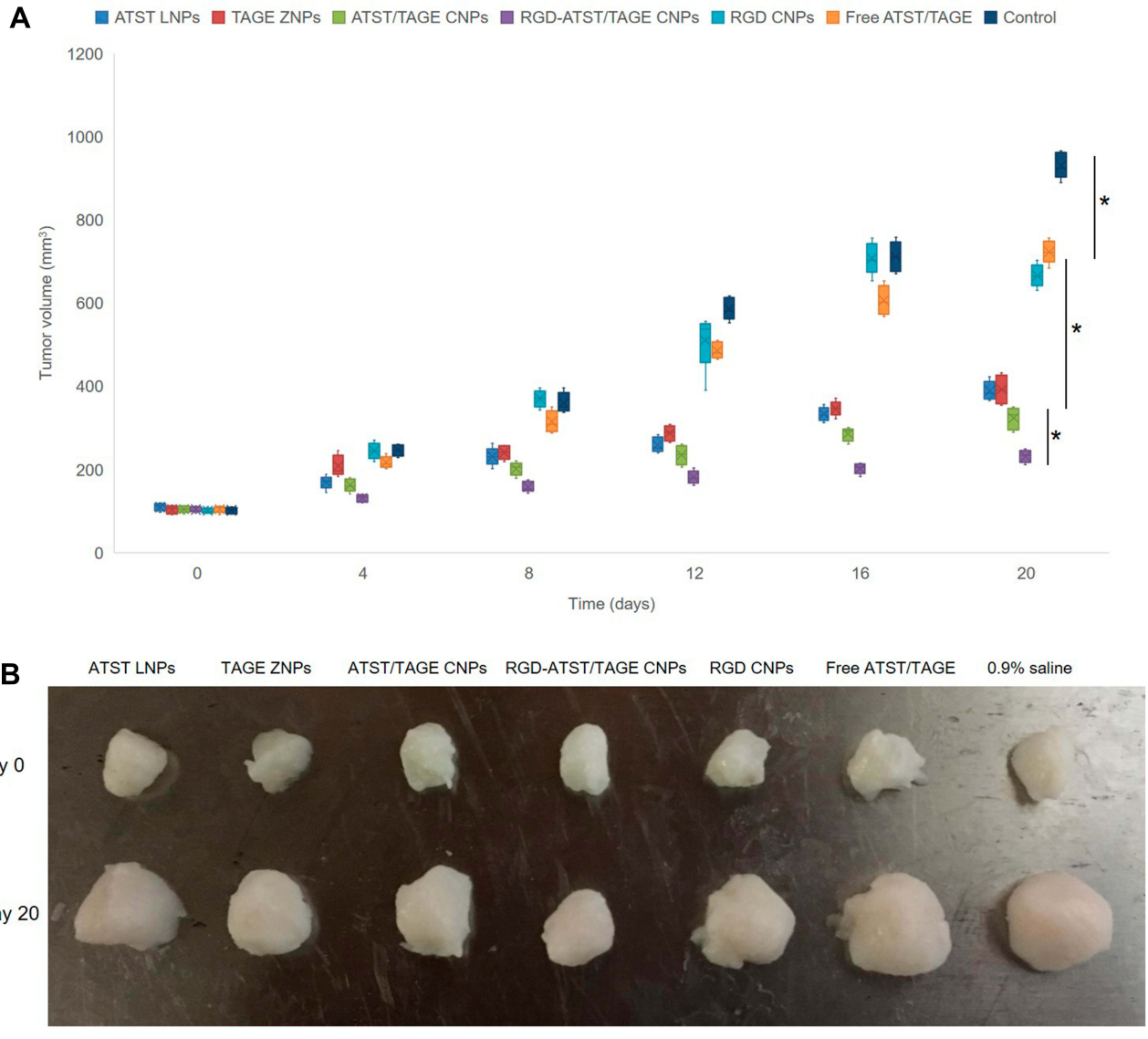

Figure 7 In vivo anti-tumor efficacy of the nano-systems was evaluated by measured and plotted the curve of tumor volume (**A**) and the tumor images (**B**) after treatment. * P<0.05.

Table 4 Tumor Inhibition Rate of Nano-Systems

Formulation	Free ATST/ TAGE	ATST LNPs	TAGE ZNPs	ATST/ TAGE CNPs	RGD-ATST/ TAGE CNPs
Tumor inhibition rate (%)	76.8	66.9	58.1	57.3	22.2

Abbreviations: ATST, atorvastatin; LNPs, lipid nanoparticles; TAGE, tangeretin; ZNPs, zein nanoparticles; RGD, arginine-glycine-aspartic; CNPs, combined nano-systems.

approach for anti-breast cancer cells strategy.[45] In this study, RGD-containing ligand was synthesized by conjugating cRGDfK with TOSD using PEG as a linker to obtain cRGDfK-PEG-TOSD. The use of PEG allows subsequent attachment of cell targeting molecules to prepare nano-systems, which retain long survival time in circulation and target recognition.[31] TOSD was used as a novel lipid to form the surface layer of the systems.[46]

A lipid nano-system: ATST LNPs, a zein nano-system: TAGE ZNPs, and ATST and TAGE combined nano-systems: ATST/TAGE CNPs and RGD-ATST/TAGE CNPs were prepared with narrow and homogenous particle size (between 102.4±3.1 and 156.9±4.1 nm, with polydispersity indexes below 0.20), which is considered as ideal for passive tumor targeting.[47] The size of nano-systems increased with RGD decoration, indicating the presence of cRGDfK-PEG-TOSD enlarged the diameters of the particles.[48] Drug entrapment efficiencies of nano-systems were high (around 90%), suggesting the good loading capacity.[49] The release profiles of ATST or TAGE from ATST LNPs and TAGE ZNPs followed zero order kinetics which indicated that the drug release is independent of the drug concentration.[50] Drugs released from RGD-ATST/TAGE CNPs followed the Higuchi model, indicating drug release by diffusion.[51] Faster release of ATST was found than that of TAGE from ATST/TAGE CNPs, which could be explained by the fact that ATST was in the outer layer of the nano-system and will be released earlier.

Cytotoxicities of both nano-systems and free drugs exhibited a dose dependent manner on both HT-29 cells and CCD-18 cells. Formulations showed different effects on HT-29 cells but similar effects on CCD-18 cells. RGD decorated nano-systems showed obvious cytotoxicity on HT-29 cells than undecorated nano-systems, but no obvious difference was found on normal CCD-18 cells. This could be the evidence that RGD may enhance the target ability of the nano-system thus gain better tumor cell inhibition effects.[52] When combination therapy is used in cancer chemotherapy, evaluation of the synergistic effect is important and CI analyses are one of the most reliable methods.[53] CI values were determined using the Chou and Talalay method to validate the synergistic effect of drugs combined in the nano-systems. The strongest synergism was observed when the weight ratio of ATST to TAGE was 1:1.

In vivo biodistribution of RGD-ATST/TAGE CNPs in the tumor site is higher than ATST/TAGE CNPs and free ATST/TAGE and opposite results were found in the heart and kidney. Similar results were reported by Wang et al.[54] These results may be explained by the fact that RGD decorated nano-systems could quickly transfer the drugs to the tumor tissue and avoid high accumulation in the heart and kidney. These results were in accordance with the findings of Yu et al.[55] The blood concentration-time profiles showed that free drugs were rapidly removed from the circulation in comparison with the nano-systems. The drugs concentration remained high in the blood for a longer period of time when they were carried by nanoparticles. The most significant efficiency of RGD-ATST /TAGE CNPs and ATST/TAGE CNPs to remain the drugs concentrations may be helpful for the long time therapeutic effects in vivo.[56] Larger AUC of RGD-ATST/TAGE CNPs than that for ATST/TAGE CNPs indicated the efficiency of drugs was significantly improved when loading with a RGD decorated nano-system. The significant increase in half-life indicates that the elimination of nano-systems was slower and that the circulation time was longer than free drugs, which was attributed to the presence of a PEG chain on the surface of particles, which provided stealth effect to the nano-systems.

In vivo tumor growth was more prominently inhibited by RGD-ATST/TAGE CNPs than ATST LNPs and TAGE ZNPs, which could be the evidence needed that combined drugs loaded nano-systems could be synergetic in the treatment of lung cancer in vivo.[57] Improved anticancer activity of RGD-ATST/TAGE CNPs was obtained compared to the ATST/TAGE CNPs group, which could be attributed to the RGD decoration. These studies demonstrated that RGD-ATST/TAGE CNPs showed the most significant synergistic therapeutic efficacy, exhibiting no significant toxicity to major organs and tissues, and body weight of the treated mice was stable. Therefore, the combination nano-system is a promising platform for colon cancer therapy.

Conclusion

In this study, RGD-containing ligand was synthesized by conjugating cRGDfK with TOSD using PEG as a linker to obtain cRGDfK-PEG-TOSD. ATST and TAGE combined nano-systems: RGD-ATST/TAGE CNPs was prepared with narrow and homogenous particle size (156.9±4.1 nm), which is considered as ideal for tumor targeting. High drug entrapment efficiencies of RGD-ATST/TAGE CNPs were found (91.3±3.7 for ATST and 89.3±3.6% for TAGE). The strongest synergism was observed when the weight ratio of ATST to TAGE was 1:1. In vivo biodistribution of RGD-ATST /TAGE CNPs in the tumor site is high and prominently inhibited the in vivo tumor growth. The combination nano-system is a promising platform for colon cancer therapy.

Abbreviations

ATST, atorvastatin; ATST LNPs, ATST loaded lipid nanoparticles; ATST/TAGE CNPs, ATST and TAGE combined nano-systems; CBP, Carbopol 940; CI, combination index; CRC, colorectal cancer; cRGDfK, cyclo (Arg-Gly-Asp-d-Phe-Lys); DCC, dicyclohexylcarbodiimide; DMEM, Dulbecco's modified Eagle's medium; FBS, Fetal bovine serum; GMS, glyceryl monostearate; ^{1}H NMR, nuclear magnetic resonance; MDR, multidrug resistance; MTT, 3-(4,5-dimethylthiazole-2-yl) −2,5-diphenyltetrazolium bromide; NCCN, National Comprehensive Cancer Network; PEG, polyethylene glycol; RGD, cyclized arginine-glycine-aspartic acid sequences; RGD-ATST/TAGE CNPs, RGD modified, ATST and TAGE combined nano-systems; RGD CNPs, blank RGD modified, ATST and TAGE combined nano-systems; TAGE, tangeretin; TOSD, D-α-tocopheryl succinate dichloromethane; TAGE ZNPs, TAGE loaded zein nanoparticles.

Funding

This research was funded by the Natural Science Basic Research Program of Shaanxi Province (Program No. 2020JQ-932).

Disclosure

The authors report no conflicts of interest in this work.

References

1. Arnold M, Sierra MS, Laversanne M, Soerjomataram I, Jemal A, Bray F. Global patterns and trends in colorectal cancer incidence and mortality. *Gut*. 2017;66(4):683–691. doi:10.1136/gutjnl-2015-310912
2. Lee WS, Yun SH, Chun HK, et al. Pulmonary resection for metastases from colorectal cancer: prognostic factors and survival. *Int J Colorectal Dis*. 2007;22(6):699–704. doi:10.1007/s00384-006-0218-2
3. Alberts SR, Horvath WL, Sternfeld WC, et al. Oxaliplatin, fluorouracil, and leucovorin for patients with unresectable liver-only metastases from colorectal cancer: a north central cancer treatment group Phase II study. *J Clin Oncol*. 2005;23(36):9243–9249. doi:10.1200/JCO.2005.07.740
4. Kemeny N. Management of liver metastases from colorectal cancer. *Oncology (Williston Park)*. 2006;20(10):1161–1176.
5. Muratore A, Zorzi D, Bouzari H, et al. Asymptomatic colorectal cancer with un-resectable liver metastases: immediate colorectal resection or up-front systemic chemotherapy? *Ann Surg Oncol*. 2007;14(2):766–770. doi:10.1245/s10434-006-9146-1
6. Hou X, Yang C, Zhang L, et al. Killing colon cancer cells through PCD pathways by a novel hyaluronic acid-modified shell-core nanoparticle loaded with RIP3 in combination with chloroquine. *Biomaterials*. 2017;124:195–210. doi:10.1016/j.biomaterials.2016.12.032
7. Kotelevets L, Chastre E, Desmaële D, Couvreur P. Nanotechnologies for the treatment of colon cancer: from old drugs to new hope. *Int J Pharm*. 2016;514(1):24–40. doi:10.1016/j.ijpharm.2016.06.005
8. Palko-Labuz A, Sroda-Pomianek K, Uryga A, Kostrzewa-Suslow E, Michalak K. Anticancer activity of baicalein and luteolin studied in colorectal adenocarcinoma LoVo cells and in drug-resistant LoVo/Dx cells. *Biomed Pharmacother*. 2017;88:232–241. doi:10.1016/j.biopha.2017.01.053
9. Chirumbolo S, Bjørklund G, Lysiuk R, Vella A, Lenchyk L, Upyr T. Targeting cancer with phytochemicals via their fine tuning of the cell survival signaling pathways. *Int J Mol Sci*. 2018;19(11):3568. doi:10.3390/ijms19113568
10. Mohana S, Ganesan M, Agilan B, et al. Screening dietary flavonoids for the reversal of P-glycoprotein-mediated multidrug resistance in cancer. *Mol Biosyst*. 2016;12(8):2458–2470. doi:10.1039/C6MB00187D
11. Wesołowska O, Wiśniewski J, Sroda-Pomianek K, et al. Multidrug resistance reversal and apoptosis induction in human colon cancer cells by some flavonoids present in citrus plants. *J Nat Prod*. 2012;75(11):1896–1902. doi:10.1021/np3003468
12. Pereira CV, Duarte M, Silva P, et al. Polymethoxylated flavones target cancer stemness and improve the antiproliferative effect of 5-fluorouracil in a 3D cell model of colorectal cancer. *Nutrients*. 2019;11(2):326. doi:10.3390/nu11020326
13. Silva I, Estrada MF, Pereira V, et al. Polymethoxylated flavones from orange peels inhibit cell proliferation in a 3D cell model of human colorectal cancer. *Nutr Cancer*. 2018;70(2):257–266. doi:10.1080/01635581.2018.1412473
14. Zheng J, Shao Y, Jiang Y, et al. Tangeretin inhibits hepatocellular carcinoma proliferation and migration by promoting autophagy-related BECLIN1. *Cancer Manag Res*. 2019;11:5231–5242. doi:10.2147/CMAR.S200974
15. Morley KL, Ferguson PJ, Koropatnick J. Tangeretin and nobiletin induce G1 cell cycle arrest but not apoptosis in human breast and colon cancer cells. *Cancer Lett*. 2007;251(1):168–178. doi:10.1016/j.canlet.2006.11.016
16. Elhennawy MG, Lin HS. Determination of tangeretin in rat plasma: assessment of its clearance and absolute oral bioavailability. *Pharmaceutics*. 2017;10(1):3. doi:10.3390/pharmaceutics10010003
17. Rizwanullah M, Amin S, Mir SR, Fakhri KU, Rizvi MMA. Phytochemical based nanomedicines against cancer: current status and future prospects. *J Drug Target*. 2018;26(9):731–752. doi:10.1080/1061186X.2017.1408115
18. Moroi M, Nagayama D, Hara F, et al. Outcome of pitavastatin versus atorvastatin therapy in patients with hypercholesterolemia at high risk for atherosclerotic cardiovascular disease. *Int J Cardiol*. 2020;305:139–146. doi:10.1016/j.ijcard.2020.01.006
19. Gambhire VM, Salunkhe SM, Gambhire MS. Atorvastatin-loaded lipid nanoparticles: antitumor activity studies on MCF-7 breast cancer cells. *Drug Dev Ind Pharm*. 2018;44(10):1685–1692. doi:10.1080/03639045.2018.1492605

20. Wu X, Song M, Qiu P, et al. Synergistic chemopreventive effects of nobiletin and atorvastatin on colon carcinogenesis. *Carcinogenesis*. 2017;38(4):455–464. doi:10.1093/carcin/bgx018
21. Xiao H, Zhang Q, Lin Y, Reddy BS, Yang CS. Combination of atorvastatin and celecoxib synergistically induces cell cycle arrest and apoptosis in colon cancer cells. *Int J Cancer*. 2008;122 (9):2115–2124. doi:10.1002/ijc.23315
22. Lee SJ, Lee I, Lee J, Park C, Kang WK. Statins, 3-hydroxy-3-methyl-glutaryl coenzyme A reductase inhibitors, potentiate the anti-angiogenic effects of bevacizumab by suppressing angiopoietin2, BiP, and Hsp90α in human colorectal cancer. *Br J Cancer*. 2014;111(3):497–505. doi:10.1038/bjc.2014.283
23. Shan D, Li J, Cai P, et al. RGD-conjugated solid lipid nanoparticles inhibit adhesion and invasion of αvβ3 integrin-overexpressing breast cancer cells. *Drug Deliv Transl Res*. 2015;5(1):15–26. doi:10.1007/s13346-014-0210-2
24. Zhu S, Qian L, Hong M, Zhang L, Pei Y, Jiang Y. RGD-modified PEG-PAMAM-DOX conjugate: in vitro and in vivo targeting to both tumor neovascular endothelial cells and tumor cells. *Adv Mater*. 2011;23(12):H84–9. doi:10.1002/adma.201003944
25. Bi W, Li X, Bi Y, et al. Novel TEMPO-PEG-RGDs conjugates remediate tissue damage induced by acute limb ischemia/reperfusion. *J Med Chem*. 2012;55(9):4501–4505. doi:10.1021/jm201381w
26. Li J, Zhang X, Wang M, et al. Synthesis of a bi-functional dendrimer-based nanovehicle co-modified with RGDyC and TAT peptides for neovascular targeting and penetration. *Int J Pharm*. 2016;501(1–2):112–123. doi:10.1016/j.ijpharm.2016.01.068
27. Yuan Z, Yuan Y, Han L, et al. Bufalin-loaded vitamin E succinate-grafted-chitosan oligosaccharide/RGD conjugated TPGS mixed micelles demonstrated improved antitumor activity against drug-resistant colon cancer. *Int J Nanomedicine*. 2018;13:7533–7548. doi:10.2147/IJN.S170692
28. Nik ME, Malaekeh-Nikouei B, Amin M, et al. Liposomal formulation of galbanic acid improved therapeutic efficacy of pegylated liposomal doxorubicin in mouse colon carcinoma. *Sci Rep*. 2019;9 (1):9527. doi:10.1038/s41598-019-45974-7
29. Han S, Sun R, Su H, et al. Delivery of docetaxel using pH-sensitive liposomes based on D-α-tocopheryl poly(2-ethyl-2-oxazoline) succinate: comparison with PEGylated liposomes. *Asian J Pharm Sci*. 2019;14(4):391–404. doi:10.1016/j.ajps.2018.07.005
30. Yu W, Liu C, Ye J, Zou W, Zhang N, Xu W. Novel cationic SLN containing a synthesized single-tailed lipid as a modifier for gene delivery. *Nanotechnology*. 2009;20(21):215102. doi:10.1088/0957-4484/20/21/215102
31. Zeng S, Wu F, Li B, et al. Synthesis, characterization, and evaluation of a novel amphiphilic polymer RGD-PEG-Chol for target drug delivery system. *ScientificWorldJournal*. 2014;2014:546176. doi:10.1155/2014/546176
32. Yu W, Liu C, Liu Y, Zhang N, Xu W. Mannan-modified solid lipid nanoparticlesfor targeted gene delivery to alveolar macrophages. *Pharm Res*. 2010;27(8):1584–1596. doi:10.1007/s11095-010-0149-z
33. Chen J, Zheng J, McClements DJ, Xiao H. Tangeretin-loaded protein nanoparticles fabricated from zein/β-lactoglobulin: preparation, characterization, and functional performance. *Food Chem*. 2014;158:466–472. doi:10.1016/j.foodchem.2014.03.003
34. Gawde KA, Sau S, Tatiparti K, et al. Paclitaxel and di-fluorinated curcumin loaded in albumin nanoparticles for targeted synergistic combination therapy of ovarian and cervical cancers. *Colloids Surf B Biointerfaces*. 2018;167:8–19. doi:10.1016/j.colsurfb.2018.03.046
35. Mathur M, Devi Vemula K. Investigation of different types of nano drug delivery systems of atorvastatin for the treatment of hyperlipidemia. *Drug Dev Ind Pharm*. 2018;44(12):2048–2060. doi:10.1080/03639045.2018.1508225
36. Li W, Weu Y, Zhao Y, Zhang S, Liu F, Yang L. Content determination of polymethoxylated favones in pericarpium citri reticulatae from different cultivar origins by HPLC. *China Pharm*. 2019;13:30–32.
37. Ortiz R, Cabeza L, Arias JL, et al. Poly(butylcyanoacrylate) and poly (ε-caprolactone) nanoparticles loaded with 5-fluorouracil increase the cytotoxic effect of the drug in experimental colon cancer. *AAPS J*. 2015;17(4):918–929. doi:10.1208/s12248-015-9761-5
38. Tian L, Qiao Y, Lee P, et al. Antitumor efficacy of liposome-encapsulated NVP-BEZ 235 in combination with irreversible electroporation. *Drug Deliv*. 2018;25(1):668–678. doi:10.1080/10717544.2018.1444683
39. Chou TC, Talaly P. A simple generalized equation for the analysis of multiple inhibitions of Michaelis-Menten kinetic systems. *J Biol Chem*. 1977;252(18):6438–6442.
40. Palko-Łabuz A, Środa-Pomianek K, Wesołowska O, Kostrzewa-Susłow E, Uryga A, Michalak K. MDR reversal and pro-apoptotic effects of statins and statins combined with flavonoids in colon cancer cells. *Biomed Pharmacother*. 2019;109:1511–1522. doi:10.1016/j.biopha.2018.10.169
41. Miyazawa T, Nakagawa K, Harigae T, et al. Distribution of β-carotene-encapsulated polysorbate 80-coated poly(D, L-lactide-co-glycolide) nanoparticles in rodent tissues following intravenous administration. *Int J Nanomedicine*. 2015;10:7223–7230. doi:10.2147/IJN.S94336
42. Guan X, Zheng X, Vong CT, et al. Combined effects of berberine and evodiamine on colorectal cancer cells and cardiomyocytes in vitro. *Eur J Pharmacol*. 2020;875:173031. doi:10.1016/j.ejphar.2020.173031
43. Genovese S, Epifano F, Preziuso F, et al. Gercumin synergizes the action of 5-fluorouracil and oxaliplatin against chemoresistant human cancer colon cells. *Biochem Biophys Res Commun*. 2020;522 (1):95–99. doi:10.1016/j.bbrc.2019.11.068
44. Viale M, Tosto R, Giglio V, et al. Cyclodextrin polymers decorated with RGD peptide as delivery systems for targeted anti-cancer chemotherapy. *Invest New Drugs*. 2019;37(4):771–778. doi:10.1007/s10637-018-0711-9
45. Murugan C, Rayappan K, Thangam R, et al. Combinatorial nanocarrier based drug delivery approach for amalgamation of anti-tumor agents in breast cancer cells: an improved nanomedicine strategy. *Sci Rep*. 2016;6(1):34053. doi:10.1038/srep34053
46. Dong Y, Zhang Z, Feng SS. d-alpha-tocopheryl polyethylene glycol 1000 succinate (TPGS) modified poly(l-lactide) (PLLA) films for localized delivery of paclitaxel. *Int J Pharm*. 2008;350(1–2):166–-171. doi:10.1016/j.ijpharm.2007.08.043
47. Wickens JM, Alsaab HO, Kesharwani P, et al. Recent advances in hyaluronic acid-decorated nanocarriers for targeted cancer therapy. *Drug Discov Today*. 2017;22(4):665–680. doi:10.1016/j.drudis.2016.12.009
48. Song S, Mao G, Du J, Zhu X. Novel RGD containing, temozolomide-loading nanostructured lipid carriers for glioblastoma multiforme chemotherapy. *Drug Deliv*. 2016;23(4):1404–1408. doi:10.3109/10717544.2015.1064186
49. Hong Y, Che S, Hui B, et al. Lung cancer therapy using doxorubicin and curcumin combination: targeted prodrug based, pH sensitive nanomedicine. *Biomed Pharmacother*. 2019;112:108614. doi:10.1016/j.biopha.2019.108614
50. Cerea M, Foppoli A, Palugan L, et al. Non-uniform drug distribution matrix system (NUDDMat) for zero-order release of drugs with different solubility. *Int J Pharm*. 2020;581:119217. doi:10.1016/j.ijpharm.2020.119217
51. Akhter MH, Kumar S, Nomani S. Sonication tailored enhance cytotoxicity of naringenin nanoparticle in pancreatic cancer: design, optimization, and in vitro studies. *Drug Dev Ind Pharm*. 2020;1–41.
52. Wang C, Su L, Wu C, Wu J, Zhu C, Yuan G. RGD peptide targeted lipid-coated nanoparticles for combinatorial delivery of sorafenib and quercetin against hepatocellular carcinoma. *Drug Dev Ind Pharm*. 2016;42(12):1938–1944. doi:10.1080/03639045.2016.1185435
53. Li S, Wang L, Li N, Liu Y, Su H. Combination lung cancer chemotherapy: design of a pH-sensitive transferrin-PEG-Hz-lipid conjugate for the co-delivery of docetaxel and baicalin. *Biomed Pharmacother*. 2017;95:548–555. doi:10.1016/j.biopha.2017.08.090

54. Wang J, Su G, Yin X, et al. Non-small cell lung cancer-targeted, redox-sensitive lipid-polymer hybrid nanoparticles for the delivery of a second-generation irreversible epidermal growth factor inhibitor-Afatinib: in vitro and in vivo evaluation. *Biomed Pharmacother*. 2019;120:109493. doi:10.1016/j.biopha.2019.109493
55. Yu J, Gu Y, Du KT, Mihardja S, Sievers RE, Lee RJ. The effect of injected RGD modified alginate on angiogenesis and left ventricular function in a chronic rat infarct model. *Biomaterials*. 2009;30(5):751–756. doi:10.1016/j.biomaterials.2008.09.059
56. Wang H, Sun G, Zhang Z, Ou Y. Transcription activator, hyaluronic acid and tocopheryl succinate multi-functionalized novel lipid carriers encapsulating etoposide for lymphoma therapy. *Biomed Pharmacother*. 2017;91:241–250. doi:10.1016/j.biopha.2017.04.104
57. Zhang R, Ru Y, Gao Y, Li J, Mao S. Layer-by-layer nanoparticles co-loading gemcitabine and platinum (IV) prodrugs for synergistic combination therapy of lung cancer. *Drug Des Devel Ther*. 2017;11:2631–2642. doi:10.2147/DDDT.S143047